Molecular Crystals and Liquid Crystals
Publication details, including instructions for authors and subscription information:
http://www.tandfonline.com/loi/gmcl20

Double Hydrogen Bonded Liquid Crystals: A Study of Light Modulation and Field Induced Transition (FiT)

V. N. Vijayakumar [a] & M. L. N. Madhu Mohan [a]
[a] Liquid Crystal Research Laboratory (LCRL), Bannari Amman Institute of Technology, Sathyamangalam, India

Version of record first published: 01 Mar 2010

To cite this article: V. N. Vijayakumar & M. L. N. Madhu Mohan (2010): Double Hydrogen Bonded Liquid Crystals: A Study of Light Modulation and Field Induced Transition (FiT), Molecular Crystals and Liquid Crystals, 517:1, 113-126

To link to this article: http://dx.doi.org/10.1080/15421400903483932

Mol. Cryst. Liq. Cryst., Vol. 517: pp. 113–126, 2010

ISSN: 1542-1406 print/1563-5287 online
DOI: 10.1080/15421400903483932

Taylor & Francis
Taylor & Francis Group

Double Hydrogen Bonded Liquid Crystals: A Study of Light Modulation and Field Induced Transition (FiT)

V. N. VIJAYAKUMAR AND
M. L. N. MADHU MOHAN

Liquid Crystal Research Laboratory (LCRL), Bannari Amman Institute of Technology, Sathyamangalam, India

A novel series of double hydrogen bonded liquid crystals have been isolated. Hydrogen bond was formed between non mesogen ingredient succinic acid and mesogenic p-n alkoxy benzoic acids. Phase diagram was constructed from the transition temperatures obtained by differential scanning colorimetry (DSC) and polarizing optical microscopic (POM) studies. Thermal and electrical properties exhibited by succinic acid and nonyloxy benzoic acid (SA + 9BA) were discussed. Interesting feature of the present investigation was the observation of a field-induced transition (FiT) in SA + 9BA hydrogen bonded complex. Three threshold field values are noticed which gives rise to two new phases (E_1 and E_2) induced by external bias voltage and on further enhancement of the bias voltage the mesogen behaves like an optical shutter, thus this hydrogen bonded complex mesogen acts as an effective light modulator. It was noticed that FiT was reversible, in the sense that when applied filed was removed, the original texture was restored, theoretical modeling and experimental results were presented.

Keywords Field induced transition; hydrogen bonded liquid crystal; light modulator; SA + nBA

Introduction

Liquid Crystal (LC) materials refer to the fourth state of matter that possesses dual property of crystals and liquids. Their anisotropic physical properties (characteristic of their crystalline nature) and the inherent surface alignment (to the substrate) tendency (characteristic of its fluidity) are extensively exploited [1–3] to design LC-based Electro-Optic devices. Their overall shape [4] being cylindrical renders them readily viable for surface alignment. In the field of supramolecular LCs, especially in the field of hydrogen bonded LCs, the influence of soft-covalent interaction for the thermal stability of phases of device interest is widely [2–17] studied.

The configuration and spread of the hydrogen bonding interaction with regard to the long molecular dipole moment in the calamitic LCs along with the corresponding molecular dipole models are argued [5,7,8] to originate the distinct properties in the

Address correspondence to M. L. N. Madhu Mohan, Liquid Crystal Research Laboratory (LCRL), Bannari Amman Institute of Technology, Sathyamangalam 638-401, India. E-mail: mln.madhu@gmail.com

family of hydrogen bonded liquid crystals (HBLCs). However, an integrated overview, if achieved for the microscopic interactions among molecular dipoles as contributed by the underlying chemical moieties configured on the molecular body (or frame) would be of immense utility in devices. The field of systematic studies in the area of LCs is expected to further reveal the truth of microscopic interactions. The growth of order (and crystalline nature) is logically expected to increase with decreasing temperature in these LC materials in their condensed version of matter.

In the case of HBLCs the molecular frame possesses [10,18–22] additional soft-covalent interaction. Further, in case of non-FE and FE HBLCs, the observed [13,21] variation in device relevant properties like thermal stability, spontaneous polarization. Tilt angle, switching times, etc. are addressed through dipolar and refined dipolar models to vouch the fact that soft-covalent interaction extends rather inclined to the long molecular dipole moment. Further, the presence of additional interaction in the form of anisotropic dipole moment along the molecular body is believed to give origin to the orientational disorder leading to tilted phases.

From our previous experience [23–30] in designing, synthesizing and characterizing various types of liquid crystals, a successful attempt has been made in characterizing a novel series of inter-hydrogen bonded liquid crystal. In the present communication a homologous series of HBLC is designed in such a way that the molecule possesses double hydrogen bonding with succinic acid moiety. Thermal and electrical characterizations of mesogens pertaining to the present series are discussed in detail.

Experimental

Optical textural observations were made with a Nikon polarizing microscope equipped with Nikon digital CCD camera system with 5 mega pixels and $2560 * 1920$ pixel resolutions. The liquid crystalline textures were processed, analyzed, and stored with the aid of ACT-2U imaging software system. The temperature control of the liquid crystal cell was equipped by Instec HCS402-STC 200 temperature controller (Instec, USA) to a temperature resolution of $\pm 0.1^{\circ}C$. This unit is interfaced to the computer by IEEE –STC 200 to control and monitor the temperature. The liquid crystal sample is filled by capillary action in its isotropic state into a commercially available (Instec, USA) polyamide buffed cell with 4 micron spacer. Optical extinction technique was used for the determination of tilt angle. The transition temperatures and corresponding enthalpy values were obtained by DSC (Shimadzu DSC-60). Infrared spectroscopy (FTIR) spectra was recorded (ABB FTIR MB3000) and analyzed with the MB3000 software. The p-n-alkoxy benzoic acids (nABA) and succinic acid were supplied by Sigma Aldrich, Germany, and all the solvents used were E. Merk grade.

Synthesis of HBLC

Intermolecular hydrogen bonded mesogens are synthesized by the addition of two moles of p-n-alkoxy benzoic acids (nABA) with one mole of succinic acid in N,N-dimethyl formamide (DMF), respectively. Further, they are subject to constant stirring for 10 hours at ambient temperature of $30^{\circ}C$ till a white precipitate in a dense solution is formed. The white crystalline crude complexes so obtained by removing

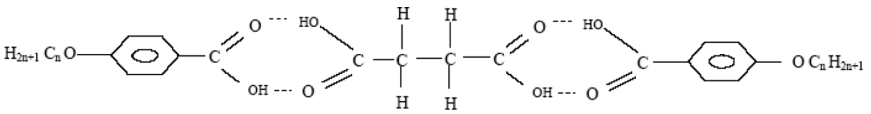

Figure 1. Molecular structure of SA + nBA inter hydrogen bonded complex.

excess DMF are then recrystallized with dimethyl sulfoxide (DMSO), and the yield varied from 85% to 95%. The molecular structure of the present homologous series of p-n-alkoxy benzoic acids with succinic acid is depicted in the Fig. 1, where n represents the alkoxy carbon number.

Results and Discussion

All the mesogens isolated under the present investigation are white crystalline solids and are stable at room temperature. They are insoluble in water and sparingly soluble in common organic solvents such as methanol, ethanol, and benzene and dicholoro methane. However, they show a high degree of solubility in coordinating solvents like DMSO, DMF, and pyridine. All these mesogens under present investigation melt at specific temperatures below 150°C. They show high thermal and chemical stability when subjected to repeated thermal scans performed during polarizing optical microscopic (POM) and DSC studies.

FTIR

Infrared (IR) spectra of free p-n-alkoxy benzoic acid, succinic acid, and their intermolecular hydrogen bonded complexes were recorded in the solid state (KBr) at room temperature. As a representative case of the homologous series, Fig. 2

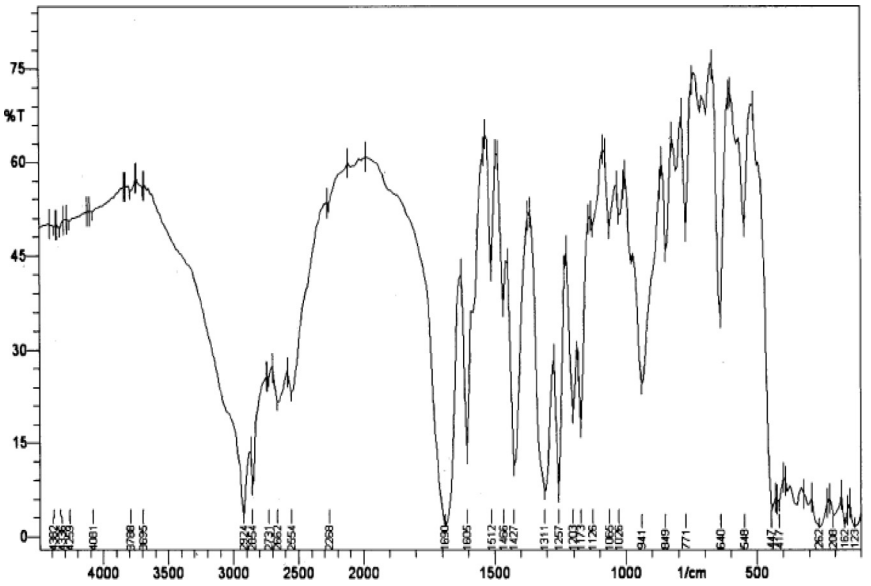

Figure 2. FTIR spectra of SA + 9BA inter hydrogen bonded complex.

illustrates the FTIR spectra of the hydrogen bonded complex of SA + 9BA in solid state at room temperature as a representative case. The solid state spectra of free alkoxybenzoic acid is reported [21] to have two sharp bands at 1685 cm^{-1} and 1695 cm^{-1} due to the frequency ν(C=O) mode. The doubling feature of this stretching mode confirms the dimeric nature of alkoxybenzoic acid at room temperature [21]. Further, in the present SA + 9BA hydrogen bonded complex, a band appearing at 2924 cm^{-1} is assigned to ν(O-H) mode of the carboxylic acid group.

The doubling nature of ν(C=O) mode may be attributed to the dimeric nature of acid group at room temperature [21]. Corresponding spectrum of solution state (chloroform) show a strong intense band suggesting the existence of monomeric form of benzoic acid. A noteworthy feature in the spectra of SA + 9BA complex is the appearance of a broad band at 1690 cm^{-1} and non-appearance of the doubling nature of ν(C=O) mode of benzoic acid moiety. This clearly suggests that the dimeric nature of the benzoic acid dissociates and prefers to exist in a monomeric form upon complexation.

Phase Identification

The observed phase variants, transition temperatures, and corresponding enthalpy values obtained by DSC in cooling and heating cycles for the SA + 9BA complexes are presented in Table 1.

SA + nBA Homologous Series

The mesogens of succinic acid and alkoxy benzoic acid homologous series are found to exhibit characteristic textures [31], viz., nematic (droplets), smectic C (schlieren texture), and smectic G (multicolored mosaic texture), respectively. The general phase sequence of the succinic acid and nonyloxy benzoic acid hydrogen bonded complexes in the cooling run can be shown as:

$$Isotropic \rightarrow N \rightarrow Sm\ C \rightarrow Sm\ G \rightarrow Crystal \quad (SA + 7BA,\ SA + 8BA,\ SA + 9BA)$$

$$Isotropic \rightarrow N \rightarrow Crystal \quad (SA + 3BA,\ SA + 5BA)$$

DSC Studies

DSC thermograms are recorded in heating and cooling cycles. The liquid crystal sample is crimped in an aluminum cell and heated with a scan rate of 10°C/min and held at its isotropic temperature for one minute so as to attain thermal stability. The cooling run is performed with a scan rate of 10°C/min. As a representative case, the DSC thermogram of SA + 9BA is illustrated in Fig. 3. The respective equilibrium transition temperatures and corresponding enthalpy values of the mesogens of the homologous series are listed separately in Table 1. Polarizing optical microscopic studies are good agreement with the DSC results.

Phase diagrams

The phase diagrams of pure p-n-alkoxybenzoic acids and the present homologous series (nBA + SA) are constructed through optical polarizing microscopic studies by

Table 1. Comparison of transition temperatures obtained by various techniques

Carbon	Phase variant	Technique	Cry-Melt	N	C	C_p	C_r	G	Cryt.
3	N	DSC (h)	137.54 (274.62)	Merged with melt	–	–	–	–	
		DSC (c)		130.43 (14.55)	–	–	–	–	127.88 (78.38)
5	N	DSC (h)	88.35 (92.37)	123.43 (17.05)	–	–	–	–	
		DSC (c)		120.09 (17.08)	–	–	–	–	83.07 (91.77)
7	NCG	DSC (h)	99.97 (93.09)	Not resolved	107.33 (5.06)			113.20 (11.84)	
		DSC (c)		110.76 (0.92)	106.86 (4.74)	–	–	92.73 (1.58)	90.17 (89.51)
8	NCG	DSC (h)	75.10 (134.26)	141.59 (32.87)	104.74 (3.77)	–	–	100.57 (80.96)	
		DSC (c)		138.01 (28.31)	100.49 (18.6)	–	–	92.57 (87.56)	52.14 (98.98)
9	NCG	DSC (h)	102.90 (171.16)	122.35 (0.99)	120.89 (22.30)			102.79 (210.27)	
		DSC (c)		Not resolved	118.10 (24.32)	–	–	97.97 (191.01)	87.5 (7.22)

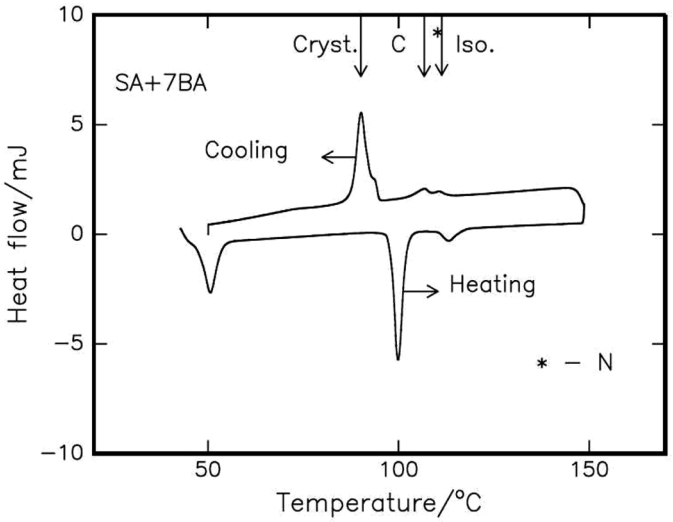

Figure 3. DSC thermogram SA + 7BA inter hydrogen bonded complex.

the phase transition temperatures observed in the cooling run of the mesogens of the present homologous series. The phase diagram of pure p-n-alkoxybenzoic acids is reported [24] to exhibit three phases namely, nematic, smectic C, and smectic G.

The phase diagram of the present homologous series of nBA + SA is shown in Fig. 4. The mesogens exhibit three phases, namely, nematic, smectic C, and smectic G. The following points are elucidated from Fig. 4:

i. The nematic phase is observed in all members of the homologous series;
ii. Thermal span of nematic phase increased up to heptyloxy carbon, while it almost remained unaltered in the other members of the homologous series;

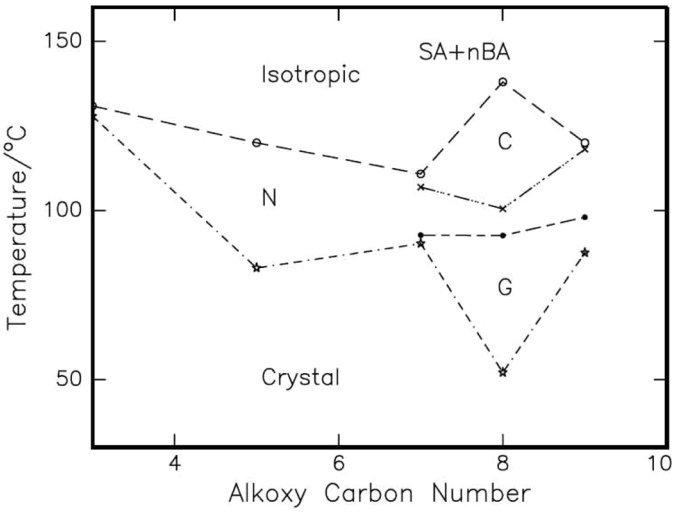

Figure 4. Phase diagram of homologous series of SA + nBA series.

iii. A tilted phase smectic C phase is induced at heptyloxy carbon. The thermal span of this phase is maximum in octyloxy carbon, while it diminished in nonyloxy carbon number;
iv. A higher ordered smectic G phase is also induced at heptyloxy carbon. The thermal span of this phase is observed to be maximum at octyloxy carbon and drastically decreased in nonyloxy carbon;
v. In totality, smectic G and C phases are induced in the higher members of homologous series.

Optical Tilt Angle Studies

For the hydrogen bonded SA + 9BA complex, optical tilt angle has been experimentally measured by optical extinction method [32] in various smectic C phases of field-induced transition (FiT) viz. E_0 and E_1. From Fig. 5, it is observed that the tilt angle increases with decreasing temperature and attains a saturation value. The saturated value of the tilt angle in E_0 and E_1 are observed to be 18° and 23°, respectively. These large magnitudes of the tilt angle are attributed [22] to the direction of the soft covalent hydrogen bond interaction which spreads along molecular long axis with finite inclination.

Tilt angle is a primary order parameter [32,33] in tilted phases viz. smectic C, the temperature variation is estimated by fitting the observed data of θ(T) to the relation

$$\theta(\mathrm{T}) \, \alpha \, (\mathrm{T} - \mathrm{T_C})^{\beta}. \tag{1}$$

The critical exponent β value estimated by fitting the data of θ(T) to the above Eq. (1) is found to be 0.50 to agree with the Mean Field [34] prediction. The dotted line in

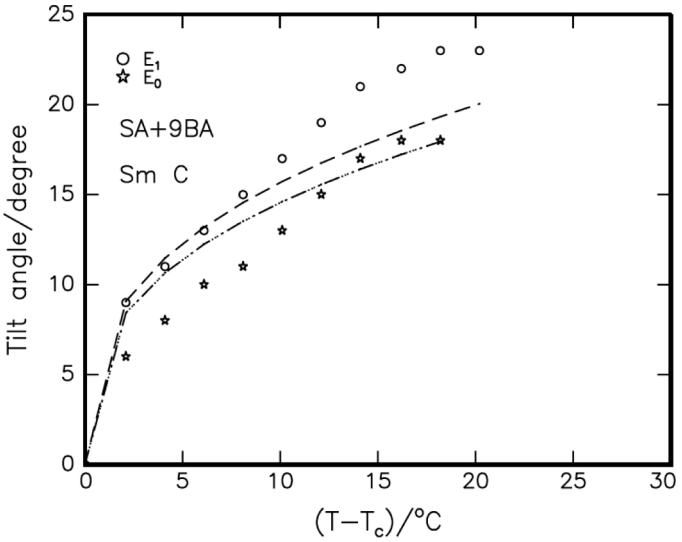

Figure 5. Temperature variation of tilt angle in smectic C phase of SA + 9BA in E_0 and E_1 FiT. Dotted line denotes the theoretical fit.

Fig. 5 depicts the fitted data. Further, the agreement of β with Mean Field value infers the long-range interaction of transverse dipole moment for the stabilization of tilted smectic C phase.

FiT

It is reported [29,35–43] that when a mesogen is subjected to an applied external field in smectic C phase, there can be a phase transition which is referred as FiT. The present homologous compounds are subjected to various strengths of external dc bias voltage derived from HP 4192A impedance analyzer, to investigate the occurrence of FiT. In the present study, two new phases referred as E_1 and E_2 are identified on application of filed.

FiT in SA + 9BA

SA + 9BA compound in its smectic C phase when an applied dc bias voltage exceeds a particular threshold value, the phase of the compound is observed to change which is referred as field induced transition. These transitions are classified as E_0, E_1, and optical shutter (E_2), each possessing different characteristic texture and threshold voltage level. Plates 1 to 3 depict the textures under the influence of applied field and along with the texture in the non conducting area. Immediately after withdrawing the bias voltage from any of the induced transition the original texture of the smectic C phase is retained. Thus this process is reversible with bias voltage. In the entire thermal span of smectic C phase ($\sim$118°C to $\sim$97°C), FiT are observed. While in the other phases preceding and succeeding smectic C phase, no such

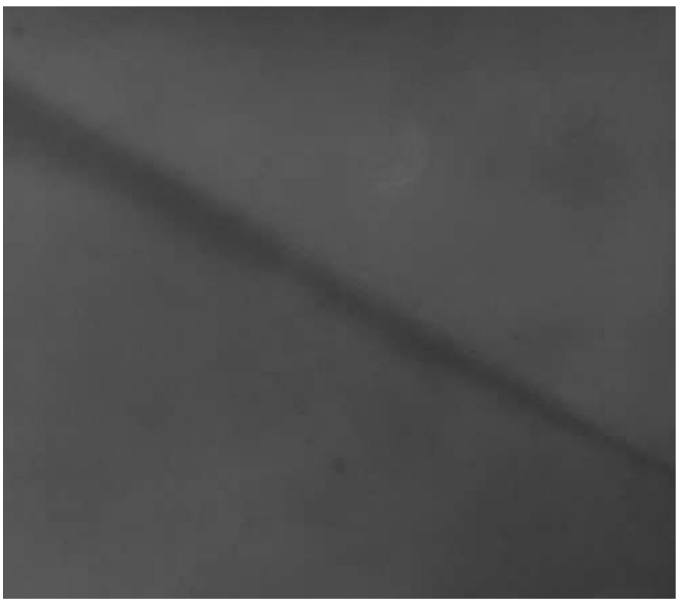

Plate 1. Optical texture of E_0 in SA + 9BA complex along with texture in the nonconducting area.

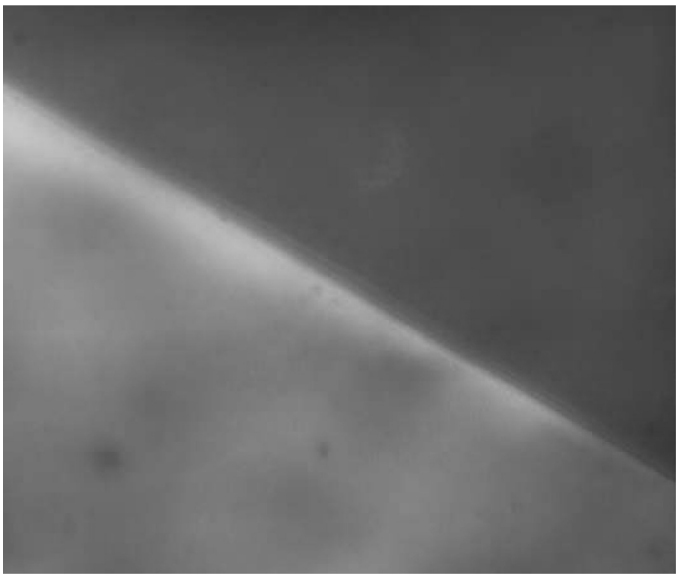

Plate 2. Optical texture of E_1 in SA + 9BA complex along with texture in the nonconducting area.

transition is found. Thus the FiT can be represented as

$$E_0 \rightarrow E_1 \rightarrow \text{Optical shutter } (E_2).$$

A quantitative approach is made to study the effect of applied electric field on hydrogen bonded SA + 9BA with optical textural studies, optical tilt, and dielectric studies.

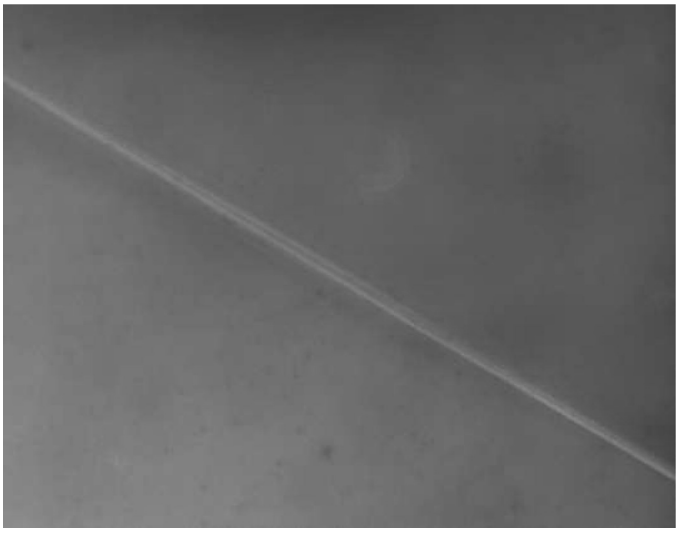

Plate 3. Optical shutter in SA + 9BA complex along with texture in the nonconducting area.

The smectic C phase with a bias voltage (both polarities) less than or equal to ±3.75 volts/micron is referred as E_0, where there is no change in the texture of the smectic phase as depicted in Plate 1.

But when a dc bias voltage of ±5.0 volts/micron is applied, the optical texture of the compound suddenly changes with change of color, this new phase is designated as E_1 which is depicted as Plate 2. The tilt angle in this phase has been studied with temperature which is shown as Fig. 5. The magnitude of the tilt angle increased with decrement in temperature and attained a saturated value of ~23° at ~99°C. Further the tilt is fitted to a power law and it is seen that the β agrees with Mean Field theory [34]. An important observation is that when the threshold value is increased beyond ±5.0 volts/micron the optical extinction is observed, which may be due to the alignment of the molecules, and is referred to as optical shutter.

To substantiate the above results, dielectric studies are performed. The variation of capacitance with respect to external bias voltage is studied in FiT phases. Such a variation for SA + 9BA compound is shown in Fig. 6. The plot depicts a symmetric variation of the capacitance on y axis with both positive and negative voltages on x axis. From Fig. 6, it can be inferred that:

a. Capacitance variation is identical for both the polarities inferring no influence of polarity;
b. Field induced transitions, i.e., $E_0 - E_1$, $E_1 - E_2$ (optical shutter), are not sudden and abrupt but smooth and uniform;
c. Frequency has no influence on the threshold values of the FiT;
d. Equilibrium states for the low and the high field are found to be distinct.

Intensity Profile of the Optical Texture in FiT

The sample SA + 9BA is filled in a commercially available buffed cell (Instec), and silver leads are drawn for contact. The intensity profile in various FiT has been experimentally analyzed by applying external bias voltage drawn from impedance

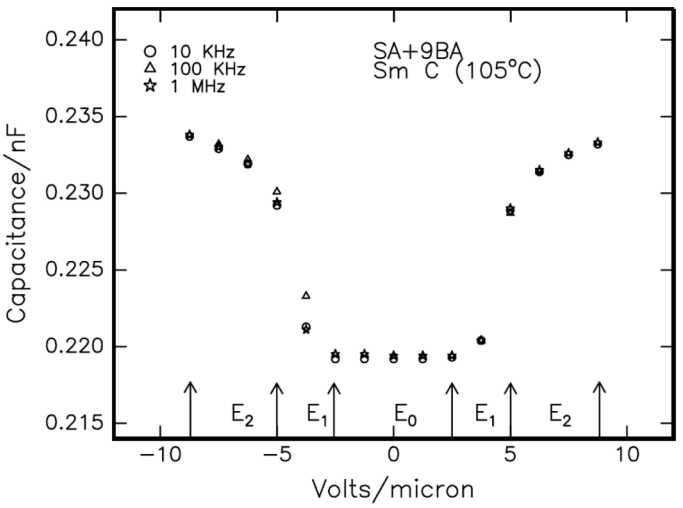

Figure 6. Capacitance variations with applied field of SA + 9BA complex.

analyzer (HP 4192A), and the intensity of the light from the liquid crystal sample is measured by a photo diode (TSL 252). As the external bias voltage is incremented in small steps. This in turn induced various FiT at different magnitudes of the applied voltage. The variation of the intensity of the texture is noted at each step of the applied bias voltage and plotted as shown in Fig. 7. It is not surprising to note that the magnitude of the light is unaltered in any of the induced transitions, namely, E_0, E_1, and E_2, respectively. But, during the transition from any one field induced transitions, there is a steep sudden decrement of the intensity of light manifesting the distortion of the helix. In the last phase of FiT, which is referred to as optical shutter, the optical profile is completely vanished. Thus the liquid crystal behaved as an optical shutter (Plate 3). Hence, this HBLC may be used as a light modulator.

Molecular Modeling of Filed-Induced Transitions

A qualitative approach for the observed FiT phenomenon is described below. Literature reports [44–50] the distortion and unwinding of the helicoidal structure with applied field in the liquid crystal mesogen. The untwisting of the helical structure of a HBLC in a thin plane layer exposed to an external action (temperature or field), and its dependence on the molecular adhesive forces at the layer boundaries are responsible for FiT. If the helical pitch is not infinite, a nonzero average polarization exists locally. When subjected to a weak electric fields the helix distorts [41] giving rise to small change in transmitted light as observed when the cell is placed under crossed polarizers. At much stronger fields there is a sudden transition such that the azimuthal orientation of the director is spatially uniform, and all layers polarization is parallel to the applied field.

For very long pitch, the liquid crystal behavior at small electric fields is expected to be different. The tilt plane of the molecules lies parallel to plane of the cell. Under these circumstances a continuous variation of the director orientation with field ($E = 0$) begins. In this region, the director profile is undisturbed. At the next level,

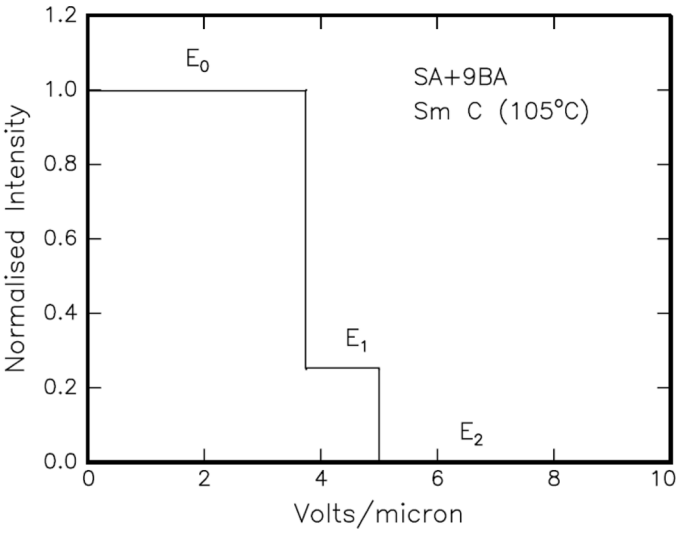

Figure 7. Optical texture intensity profile of SA + 9BA complex.

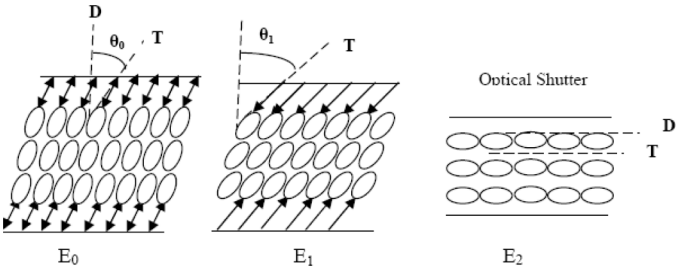

Figure 8. Molecular modeling for various FiT transitions. T denotes the tilt angle, while D denotes the director in each phase. The applied filed E is perpendicular to the cell.

i.e., $E = 1$, the electric filed is sufficient to over the elasticity possessed by the molecules. Molecules in adjacent layer undergo unequal azimuthal rotations resulting in a locally averaged nonzero polarization that couples to the electric filed. At much higher fields ($E = 2$), the distortion is more, and it helps in rapid switching, which is analogous to short helical pitch materials. The proposed molecular orientations relating to various observed FiT E_0, E_1, and optical shutter are depicted in Fig. 8. The role of the anchoring energy is considerable at low fields. As the field increases, the molecules get loosely bounded by the substrate surface. In other words, the liquid crystal behaves as a light modulator. At high fields, the extinction of the light is observed, and this state may be referred as optical shutter. The parameters like helical pitch, anchoring energy, optical tilt angle, and light modulation vary with applied field and govern the utility of the liquid crystal in display applications.

It has been experimentally observed from the tilt angle studies that the magnitude of tilt angle increases as one proceeds from the E_0 to E_1. Thus it can be concluded that the tilt angle in various field induced phase's orients depending on the strength of the applied bias. It is no surprise that the molecules prefer an alignment as shown in Fig. 8, when the bias strength is increased to a maximum value, and thus the molecules inhibits the light and act as a total optical shutter. The possible reasons for this FiT can be elicited from the various surface anchoring energy [51] possessed by the liquid crystalline molecules. When the external bias filed exceeds the surface anchoring the liquid crystalline molecule geometry prefers a orientation.

Acknowledgments

One of the authors (M. L. N. M. M.) acknowledges the financial support rendered by All India Council for Technical Education, Department of Science and Technology, and Defence Research Development Organization, New Delhi. Infrastructural support provided by Bannari Amman Institute of Technology is gratefully acknowledged.

References

[1] Meyer, R. B., Liebert, L., Strezelecki, L., & Keller, P. (1975). *J. Physique. Lett.*, *30*, 69.
[2] Kato, T. (1998). *Handbook of Liquid Crystals*, Wiley-VCH: Weinheim.
[3] Gray, G. W. (1962). *Molecular Structure and Properties of Liquid Crystals*, Academic Press: London.

[4] Kelker, H., & Hatz, R. (1980). *Handbook of Liquid Crystals*, Verlag Chemie: Weinheim.
[5] Kato, T., & Frechet, J. M. J. (1989). *J. Am .Chem. Soc.*, *111*, 8533.
[6] Yu, L. (1993). *Liq. Cryst.*, *14*, 1303.
[7] Kato, T., Kihara, H., Uryu, T., Ujiie, S., Iimura, K., Frechet, J. M. J., & Kumar, U. (1993). *Ferroelectrics*, *148*, 161.
[8] Kato, T., Uryu, T., Kaneuchi, F., Jin, C., & Frechet, J. M. J. (1993). *Liq. Cryst.*, *14*, 1311.
[9] Demus, D., Demus, H., & Zaschke, H. (1974). *Flussige Kristalle in Tabellen*, VEB Deutcher Verlag fur Grundstoffindustrie, Publisher Velag, Leipzig, Germany.
[10] Paleos, C. M., & Tsiourvas, D. (2001). *Liq. Cryst.*, *28*, 1127.
[11] Xu, B., & Swager, T. M. (1995). *J. Am. Chem. Soc.*, *117*, 5011.
[12] Malik, S., Dhal, P. K., & Mashelkar, R. A. (1995). *Macromolecules*, *28*, 2159.
[13] Sideratou, Z., Tsiourvas, D., Paleos, C. M., & Skoulios, A. (1997). *Liq. Cryst.*, *22*, 51.
[14] Goodby, J. W., Blinc, R., Clark, N. A., Lagerwall, S. T., Osipov, S. A., Pikin, S. A., Sakurai, T., Yoshino, Y., & Zecks, B. (1991). *Ferro Electric Liquid Crystal, Principles, Properties, and Applications*, U.S.A. Gorden and Breech Press: Philadalphia.
[15] Clark, N. A., & Lagerwall, S. T. (1980). *Appl. Phys. Lett.*, *36*, 899.
[16] Brand, H. R., Cladis, P. E., & Pleiner, H. (1992). *Macromol.*, *25*, 7223.
[17] Petrov, M. P., & Tsonev, L. V. (1996). *Liq. Cryst.*, *21*, 543.
[18] Kumar, P. A., Srinivasulu, M., & Pisipati, V. G. K. M. (1999). *Liq. Cryst.*, *26*, 859.
[19] Swathi, P., Kumar, P. A., & Pisipati, V. G. K. M. (2000). *Liq. Cryst.*, *27*, 665.
[20] Srinivasulu, M., Satyanarayana, P. V. V., Kumar, P. A., & Pisipati, V. G. K. M. (2001). *Liq. Cryst.*, *28*, 1321.
[21] Swathi, P., Sreehari Sastry, S., Kumar, P. A., & Pisipati, V. G. K. M. (2001). *Mol. Cryst. Liq. Cryst.*, *365*, 523.
[22] Sreedevi, B., Chalapathi, P. V., Srinivasulu, M., Pisipati, V. G. K. M., & Potukuchi, D. M. (2004). *Liq. Cryst.*, *31*, 303 and references there in.
[23] Chitravel, T., Madhu Mohan, M. L. N., & Krishnakumar, V. (2008). *Mol. Cryst. Liq. Cryst.*, *493*, 17.
[24] Vijayakumar, V. N., Murugadass, K., & Madhu Mohan, M. L. N. (2010). *Mol. Cryst. Liq. Cryst.*, 517, 41.
[25] Madhu Mohan, M. L. N., Arunachalam, B., & Arravindh Sankar, C. (2008). *Metal and Mater. Trans. A.*, *39*, 1192; Madhu Mohan, M. L. N., & Arunachalam, B. (2008). *Z. Naturforch*, *63a*, 435.
[26] Madhu Mohan, M. L. N., & Pisipati, V. G. K. M. (2000). *Liq. Cryst.*, *26*, 1609.
[27] Kumar, P. A., Madhu Mohan, M. L. N., & Pisipati, V. G. K. M. (2000). *Liq. Crys.*, *27*, 1533.
[28] Madhu Mohan, M. L. N., Kumar, P. A., Goud, B. V. S., & Pisipati, V. G. K. M. (1999). *Mater. Res. Bull.*, *34*, 2167.
[29] Madhu Mohan, M. L. N., Kumar, P. A., & Pisipati, V. G. K. M. (1999). *Ferroelectrics*, *227*, 105.
[30] Madhu Mohan, M. L. N., Potukuchi, D. M., & Pisipati, V. G. K. M. (1998). *Mol. Cryst. Liq. Cryst.*, *325*, 127.
[31] Gray, G. W., & Goodby, J. W. G. (1984). *Smetic Liquid Crystals – Textures and Structures*, Leonard Hill: London.
[32] Noot, C., Perkins, S. P., & Coles, H. J. (2000). *Ferroelectrics*, *244*, 331.
[33] de Gennes, P. G. (1974). *The Physics of Liquid Crystals*, Oxford Press: London.
[34] Stanley, H. E. (1971). *Introduction to Phase Transition and Critical Phenomena*, Oxford University Press, USA.
[35] Kobayashi, S., & Ishibashi, S. (1994). *Mol. Cryst. Liq. Cryst.*, *257*, 181.
[36] Jong-Guang, W., & Shu-Hsia, C. (1994). *Jap. Jol. Appl. Phys.*, *33*, 6249.
[37] Qian, T., & Taylor, P. L. (1999). *Phys. Rev. E.*, *60*, 2978.
[38] Napoli, G. (2006). *J. Appl. Maths.*, *71*, 34.
[39] Schlangen, L. J. M., Alexandre, P., & Cornelissen, H. J. (2000). *J. Appl. Phys.*, *87*, 3723.

[40] Hurd, A. J., Fraden, S., Lonberg, F., & Meyer, R. B. (1985). *J. de Physique*, *46*, 905.
[41] Zhang, S., Wen, B., Keast, S. S., Neubert, M. E., Taylor, P. L., & Rosenblatt, C. (2000). *Phys. Rev. Lett.*, *84*, 4140.
[42] Rotinyan, T. A., Ryumtsev, E. I., & Yazikov, S. B. (1987). *JETP Lett.*, *46*, 417.
[43] Cladiss, P. E., Garel, T., & Pieranski, P. (1986). *Phys. Rev. Lett.*, *57*, 2841.
[44] Petit, M., Daoudi, A., Ismaili, M., & Buisine, J. M. (2006). *Eur. Phys. J E Soft Matter*, *20*, 327.
[45] Abdulhalim, I., & Moddel, G. (1991). *Mol. Cryst. Liq. Cryst.*, *200*, 79.
[46] Judge, L. A., Kriezis, E. E., & Elston, S. J. (2001). *Mol. Cryst. Liq. Cryst.*, *366*, 661.
[47] Schiller, P., & Zeitler, F. (1997). *Phys. Rev. E*, *6*, 531.
[48] Schiller, P., & Zeitler, F. (1995). *J. de Physique II*, *5*, 1835.
[49] Petit, M., Daoudi, A., Ismaili, M., & Buisine, J. M. (2006). *Euro. Phys. J. E.*, *20*, 327.
[50] Belyakov, V. A. (2002). *JETP Lett.*, *76*, 88.
[51] Fazio, V. S. U., & Komitov, L. (1999). *Europhys. Lett.*, *46*, 38.